Three-dimensional cell organization leads to a different type of ionizing radiation-induced cell death: MG-63 monolayer cells undergo mitotic catastrophe while spheroids die of apoptosis

PAOLA INDOVINA[1], GABRIELLA RAINALDI[1,2] and MARIA TERESA SANTINI[1,2]

[1]Dipartimento di Ematologia, Oncologia e Medicina Molecolare, Istituto Superiore di Sanità, Viale Regina Elena 299, I-00161 Rome; [2]CNR-INFM, Unità di Napoli, Complesso Universitario Monte S. Angelo, Via Cinthia, I-80126 Naples, Italy

Received March 6, 2007; Accepted April 24, 2007

Abstract. The type of cell death occurring in the same cell line (MG-63 human osteosarcoma cells) grown in monolayer or as three-dimensional spheroids after exposure to 5 Gy of ionizing radiation was determined. Morphological analyses using the chromatin dye Hoechst 33258 demonstrated that spheroids showed the typical characteristics of apoptosis, while monolayer cells revealed those typical of mitotic catastrophe. In order to better characterize these two types of cell death, the role of caspases was examined in irradiated monolayer cells and spheroids using the broad spectrum caspase inhibitor zVAD-fmk. Death in monolayer cells was caspase-independent, whereas spheroid death was characterized by caspase dependence. Members of the Bcl-2 family of proteins and survivin involved in cell death processes were also studied by Western blot analysis. The pro-apoptotic protein Bax increased in spheroids, whereas this protein remained unchanged in monolayer cells after the same 5-Gy irradiation. The anti-apoptotic protein Bcl-2, on the other hand, remained unchanged in both monolayer cells and spheroids. Finally, survivin increased significantly after irradiation in both cells in monolayer and spheroids. The results presented suggest that three-dimensional cell organization leads to a different type of cell death after exposure to ionizing radiation. Thus, the use of spheroids, a cell model which mimics *in vivo* solid tumors more closely than cells grown in monolayer, is more appropriate when investigating the effects of antineoplastic treatments such as ionizing radiation.

Introduction

Stabilized tumor cell lines grown in monolayer have been widely used to investigate cancer. Although this *in vitro* cell model has yielded valuable information regarding the mechanisms at the basis of tumor insurgence and growth, it is, nonetheless, unsuitable in representing completely *in vivo* tumors. In fact, solid tumors grow in a three-dimensional spatial array and cells in these tumors are exposed to non-uniform distributions of oxygen and nutrients as well as to other physical and chemical stresses. Therefore, it is obvious that cells grown in monolayer, which are exposed to the same oxygen and nutrient concentrations and also have less complex cell-cell and cell-matrix interactions, cannot be utilized to study all aspects of tumor biology. Thus, in order to design more suitable *in vitro* systems that take into consideration the three-dimensional arrangement of solid tumors, multicellular tumor spheroids were developed (1,2). Indeed, tumor spheroids represent quite realistically the three-dimensional growth and organization of solid tumors and, consequently, simulate much more precisely diverse cell processes including cell death.

It has been demonstrated that ionizing radiation can induce numerous effects in cells including changes in metabolism (3), cell cycle delay (4), damage to DNA (5) and the cell membrane (6), and, ultimately, cell death (7). We have recently demonstrated using ^{1}H-NMR spectroscopy that MG-63 cells grown in monolayer and as three-dimensional spheroids have a different cell death response to 2 Gy of ionizing radiation (8). The spectra of spheroids showed metabolic variations indicative of apoptosis while those of monolayer cells did not show such changes. In addition, analyses utilizing the chromatin dye Hoechst 33258 of monolayer cells showed the morphological signs of a type of cell death known as mitotic catastrophe.

In recent years, the term 'mitotic catastrophe' has been widely used to define a type of programmed cell death that occurs during mitosis. Although there is no generally accepted definition to describe this form of cell death, numerous attempts have nonetheless been made to characterize it. For instance, from a morphological standpoint, cells undergoing mitotic catastrophe are described as cells with multiple, multilobed or abnormally large nuclei or cells with micronuclei (9,10). These characteristics are quite diverse from those noted during apoptosis. In fact, apoptotic cells have clumped or condensed nuclear chromatin and/or chromatin marginalized against the nuclear membrane (11-13). Caspase-dependence

Correspondence to: Dr Maria Teresa Santini, Dipartimento di Ematologia, Oncologia e Medicina Molecolare, Istituto Superiore di Sanità, Viale Regina Elena 299, I-00161 Rome, Italy
E-mail: santini@iss.it

Key words: three-dimensional tumor spheroid, mitotic catastrophe, apoptosis, ionizing radiation

or independence examined with caspase inhibitors such as zVAD-fmk (z-Val-Ala-Asp-fluoromethylketone) is another criterion which was used to distinguish mitotic catastrophe from apoptosis. It was believed that mitotic catastrophe was caspase-independent while apoptosis was caspase-dependent (14). However, since it is now accepted that both mitotic catastrophe and apoptosis can be either caspase-dependent or independent, this criterion cannot be used to distinguish the two types of cell death. Another possible mode of distinguishing mitotic catastrophe from apoptosis is through analysis of cell-cycle checkpoint dysregulation (15). In fact, mitotic catastrophe results from a combination of deficient cell-cycle checkpoints (i.e., the G2/M checkpoint and the spindle assembly checkpoint) and cellular damage. Failure to arrest the cell cycle after damage to the structure of DNA and the mitotic spindle before mitosis triggers aberrant chromosome segregation and mitotic catastrophe.

Cell cycle checkpoint regulation also involves survivin. In particular, survivin is a substrate for Cdk1 during the G2/M phase of the cell cycle and contributes to spindle checkpoint regulation by binding to tubulin on the mitotic spindle (16-18). In addition, survivin is also a member of the inhibitor of apoptosis protein (IAP) gene family and suppresses caspase activation possibly by binding to the caspase activator Smac/DIABLO (19). It has been shown that an antisense oligonucleotide directed against survivin induced caspase-independent mitotic catastrophe in a neuroblastoma cell line, while the same oligonucleotide caused caspase-dependent apoptosis in an oligodendroglioma cell line (20). Thus, survivin can be involved in both caspase-dependent and independent cell death processes.

Understanding the possible role of the Bcl-2 family of apoptotic proteins such as Bax, Bcl-2 and Bcl-X_L in relation to mitotic catastrophe is also of extreme importance although many studies have yielded conflicting results. In particular, it has been demonstrated that overexpression of the anti-apoptotic Bcl-2 protein in etoposide-treated HeLa cells increases the insurgence of mitotic catastrophe (21). These results seem to suggest that the role of the Bcl-2 family of proteins is quite different in mitotic catastrophe and apoptosis since an anti-apoptotic protein actually increases cell death through mitotic catastrophe. In addition, no changes in Bax and Bcl-2 were observed in combretastin-A4 prodrug-induced mitotic catastrophe in the CLL cell line (14), indicating that the Bcl-2 family of proteins again behaves differently in the two types of cell death. Conversely, other investigators have shown that the Bcl-2 family of proteins carry out a similar role in apoptosis and mitotic catastrophe. For instance, transfection with the anti-apoptotic Bcl-2 and Bcl-X_L proteins or knock out of the pro-apoptotic Bax protein can prevent mitotic catastrophe (15). Also, it has been demonstrated that inhibition of Bcl-2 expression by antisense oligonucleotides can amplify mitotic catastrophe (22).

It was the purpose of the present study to determine if MG-63 cells grown in monolayer or as three-dimensional spheroids undergo a different type of cell death after exposure to 5 Gy of ionizing radiation, as was suggested in our previous ^{1}H-NMR study (8). Morphological analyses using the chromatin dye Hoechst 33258 demonstrated that spheroids show the typical characteristics of apoptosis, while monolayer cells reveal those typical of mitotic catastrophe. In order to better characterize these two types of cell death, the role of caspases was examined in irradiated monolayer cells and spheroids using the broad spectrum caspase inhibitor zVAD-fmk. Death in monolayer cells was caspase-independent, whereas spheroid death was characterized by caspase dependence. Members of the Bcl-2 family of proteins and survivin involved in cell death processes were also studied by Western blot analysis. The pro-apoptotic protein Bax increased in spheroids, whereas this protein remained unchanged in monolayer cells after the same 5-Gy irradiation. The anti-apoptotic protein Bcl-2, on the other hand, remained unchanged in both monolayer cells and spheroids. Finally, survivin increased significantly after irradiation in both monolayers and spheroids. The results presented suggest that three-dimensional cell organization leads to a different type of cell death after exposure to ionizing radiation.

Materials and methods

Cell culture conditions. MG-63 cells (a human osteosarcoma cell line) purchased from the Istituto Zooprofilattico Sperimentale della Lombardia e dell'Emilia (Brescia, Italy) were grown in monolayer in tissue culture flasks (Nunc A/S, Roskilde, Denmark) containing RPMI-1640 (Gibco BRL, Burlington, Canada) supplemented with 10% heat-inactivated fetal bovine serum (FBS Characterized; Hyclone, USA), non-essential amino acids, penicillin and streptomycin and incubated at 37˚C in a 5% CO_2 atmosphere. Aliquots of the same batch of frozen cells were thawed and used for all experiments at about the same number of passages (between 10 and 15 passages).

Spheroids. In order to form spheroids by using the liquid-overlay technique, MG-63 cells grown in monolayer were detached from the substratum by using 10 mM EDTA and 0.25% trypsin solutions. The cells were then seeded in 6-well tissue culture plates (Nunc) to which 3% agar dissolved in complete medium (RPMI plus 10% FBS) had previously been added to the bottom of the wells and had solidified. To each well $1.25x10^5$ cells/ml ($5.0x10^5$ cells/well) were added and the plates were incubated in a Steri-Cult 200 incubator (Forma Scientific, Milan, Italy) at 37˚C in a 5% CO_2 atmosphere. All products not specified were purchased from Sigma Chemical Co. (St. Louis, MO, USA).

Irradiation protocol. Both MG-63 cells and spheroids were irradiated after 24 h of growth with the doses specified directly in the tissue culture plates at room temperature using a Cobalt-60 irradiation unit (Gammacell 220, Atomic Energy of Canada Ltd.) at a dose rate of ~1.9 Gy/min. Control cultures were kept at room temperature under the same conditions as experimental ones. Cells and spheroids were collected immediately after irradiation and at 24, 48 and 72 h after irradiation.

Growth curves. In order to determine monolayer and spheroid cell proliferation, monolayer cells were seeded at $5.0x10^4$ cells/ml (total cell number was $5.0x10^5$ in 10 ml) in 100-mm diameter Petri dishes (Nunc) while spheroids were seeded

as described above. After 24 h of growth, cells and spheroids were irradiated with 5 Gy and collected at 24, 48 and 72 h after irradiation. Spheroids were disaggregated and the number of cells from these spheroids and from monolayers were counted using a Neubauer chamber. The cells were also checked for cell vitality by using the trypan blue exclusion test. Non-irradiated monolayers and spheroids, collected immediately before irradiation and at 24, 48 and 72 h after irradiation, were considered as controls.

Analysis of cell death by the nuclear dye Hoechst 33258. At 24, 48 and 72 h after exposure to ionizing radiation, MG-63 monolayer cells were fixed with 3% paraformaldehyde in PBS for 15 min, permeabilized with 0.5% Triton X-100 in PBS for 5 min and incubated with 1 μg/ml Hoechst 33258 (Sigma) for 30 min at 37˚C. Irradiated spheroids were collected at the same time-points and disaggregated with 10 mM EDTA and 0.25% trypsin at 37˚C. The single cell suspensions obtained were fixed with 3% paraformaldehyde in PBS for 15 min. The cell pellets were then placed on polylysine-coated coverslips and allowed to adhere for 20 min, permeabilized with 0.5% Triton X-100 in PBS for 5 min and incubated with 1 μg/ml Hoechst 33258 for 30 min at 37˚C. All the samples were observed with a Zeiss Axiovert fluorescence microscope (Carl Zeiss, S.p.A., Milan, Italy). The percentage of abnormal nuclei was determined by counting at high magnification (x320) at least 1000 cells of each sample in randomly selected areas. In order to distinguish apoptotic and necrotic cells, the nuclear morphological and ultrastructural parameters typical of these two kinds of cell death were taken into account (11-13). In particular, cells were considered apoptotic if their nuclei had clumped or condensed nuclear chromatin, whereas they were counted as necrotic if they had shrunken and/or disintegrated chromatin. In addition, abnormal nuclei presenting the typical morphology of mitotic catastrophe (multiple, multilobed or abnormally large nuclei or micronuclei) (9,10) were also counted.

Cell survival analyses by cellular clonogenicity experiments. Both monolayer cells and spheroids were irradiated with either 1, 2, 3, 4, 5, 6 or 8 Gy. Immediately after irradiation, MG-63 monolayer cells were detached from the tissue culture plates and spheroids were disaggregated by adding 10 mM EDTA and 0.25% trypsin at 37˚C and by pipetting. Complete medium was added and the single cell suspensions obtained were counted. Aliquots of various dilutions of cells were transferred in triplicate into 60-mm Petri dishes (Nunc). Cells were incubated at 37˚C for 15 days. After incubation, fixed colonies were stained with Giemsa and those consisting of more than 50 cells were counted. Experiments were repeated three times.

Caspase-3 enzymatic activity. MG-63 monolayer cells and spheroids irradiated with 5 Gy were collected after 24, 48 and 72 h from irradiation. Untreated controls were collected at the same time-points. Caspase-3 enzymatic activity was determined in cellular lysate (100 μg of protein per sample) using the Colorimetric Caspase-3 Assay Kit (Sigma, Product Code CASP-3-C) following the manufacturer's instructions. This assay is based on the hydrolysis of the peptide substrate acetyl-Asp-Glu-Val-Asp p-nitroanilide (Ac-DEVD-p-NA) by caspase-3, resulting in the release of the p-nitroaniline (pNA) moiety. The absorbance of pNA was measured spectrophotometrically at 405 nm by using a microplate reader.

Treatment with the caspase inhibitor zVAD-fmk. In order to examine if irradiation-induced cell death could be blocked by the inhibition of caspase activity, both MG-63 monolayer cells and spheroids were cultured in medium containing the broad-spectrum caspase inhibitor zVAD-fmk at the concentration of 40 μM. At 72 h after irradiation with 5 Gy, monolayer cells and the cells from disaggregated spheroids were counted, checked for cell vitality by using the trypan-blue exclusion test and stained with Hoechst 33258 as described above.

Western blotting. In order to determine the total Bax, Bcl-2 and survivin content in both MG-63 monolayer cells and spheroids in control conditions and after 24, 48 and 72 h from irradiation with a dose of 5 Gy, Western blot analysis was conducted. MG-63 cells and spheroids were washed twice in PBS and lysed in RIPA buffer (PBS containing 1% Igepal CA-630, 0.5% sodium deoxycholate, 0.1% SDS, 0.1 mg/ml PMSF and protease inhibitor cocktail) for 30 min on ice. The lysates were centrifuged at 10,000 g for 10 min at 4˚C and the pellets were discarded. Protein analysis was conducted by the DC protein assay kit (Bio-Rad Laboratories, Milan, Italy) using BSA as standard. Equal amounts of protein (40 μg) per sample were separated onto a 15% acrylamide gel and electroblotted onto PVDF membranes (Bio-Rad). After electroblotting the membranes were blocked with 5% non-fat dry milk (Bio-Rad) in TBST (0.1 M Tris base, 0.15 M NaCl, 0.05% Tween-20, pH 7.4) and then incubated with the primary mouse monoclonal antibodies against Bax, Bcl-2 and the primary rabbit polyclonal antibody against survivin (Santa Cruz Biotechnology, Milan, Italy) for 2 h at room temperature. Following incubation with an HRP-linked whole anti-mouse or anti-rabbit antibody (Amersham Biosciences, Milan, Italy), visualization of the bound antibody was performed with the Supersignal West Pico Chemiluminescent Substrate (Pierce, Rockford, IL, USA). The blots were exposed to X-ray film (Amersham) and then scanned using an Epson scanner. Experiments were repeated three times. An equal loading of proteins was confirmed by utilizing the primary mouse antibody against ß-actin as control (Chemicon, Milan, Italy).

Statistical analyses. All statistical analyses were carried out using the paired Student's t-test.

Results

Growth curves. Cell proliferation in monolayer cells and spheroids was determined by growth curves as described in Materials and methods. The cell numbers represent the means and standard deviations of at least 3 separate experiments (Fig. 1). As can be seen, control monolayer cells grow much more rapidly than control spheroids. In addition, it is also evident that a 5-Gy irradiation is much more efficacious in slowing down growth in monolayer cells than in spheroids, especially at 72 h.

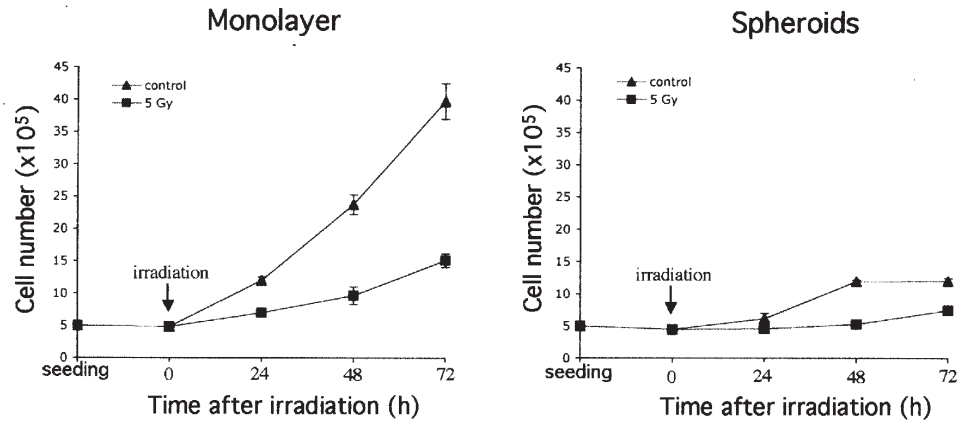

Time after irradiation (h)	Monolayer		Spheroids	
	Control (x10^5)	5 Gy (x10^5)	Control (x10^5)	5 Gy (x10^5)
0	4.82±0.03		4.46±0.69	
24	12.00±0.53	6.97±0.32	6.15±0.85	4.57±0.74
48	23.74±1.54	9.67±1.38	11.92±0.21	5.25±0.21
72	39.7±2.75	15.15±1.06	12.00±0.42	7.42±0.11

Figure 1. Growth curves of control and 5-Gy-irradiated MG-63 monolayer cells and control and 5-Gy-irradiated spheroids of the same cell line. The difference in cell proliferation is much more evident between control and irradiated monolayer cells than between control and irradiated spheroids at all times tested (24, 48 and 72 h after irradiation). The values in the curves and in the table represent the means and standard deviations of three separate experiments.

Analysis of cell death by the nuclear dye Hoechst 33258. In order to analyze the nuclear morphological characteristics of MG-63 cells and spheroids at 24, 48 and 72 h after exposure to 5 Gy of ionizing radiation, the nuclear chromatin dye Hoechst 33258 was used. In Fig. 2 are shown representative fluorescence micrographs of (a) control and (b) irradiated MG-63 monolayer cells at 72 h after irradiation, and (c) control and (d) irradiated MG-63 spheroids collected and disaggregated at this same time-point. As can be seen in Fig. 2a and c, the nuclei have uncondensed and uniformly and homogeneously distributed chromatin, characteristics typical of control cells. On the other hand, the irradiated monolayer cells shown in Fig. 2b reveal the typical morphology of mitotic catastrophe (i.e., multiple, multilobed or abnormally large nuclei or micronuclei) (9,10). In the disaggregated spheroid cells shown in Fig. 2d, the nuclear morphological and ultrastructural parameters typical of apoptosis were observed (11-13). In particular, cells were considered apoptotic if their nuclei had clumped or condensed nuclear chromatin. The percentage of monolayer cells undergoing mitotic catastrophe as well as apoptotic spheroid cells are shown in the table at the top of Fig. 2. As shown, the percentage of nuclei in monolayer cells exhibiting the characteristics of mitotic catastrophe increases with time after irradiation reaching a maximum of about 64% at 72 h. In addition, the percentage of apoptotic nuclei in spheroid cells also increases with time after irradiation reaching a maximum of about 29% at 72 h. It should also be pointed out that the percentage of apoptotic nuclei in monolayer cells undergoing mitotic catastrophe was found to be <1% at all times tested and that the percentage of nuclei with characteristics of mitotic catastrophe reached a maximum of 4% at 72 h in spheroids undergoing apoptosis. Cells with shrunken and/or disintegrated chromatin typical of necrosis were <1% in all samples at all times tested.

Cell survival analyses. In order to compare the long-term radiosensitivity of MG-63 monolayer cells and spheroids, cellular clonogenicity experiments were conducted. The plating efficiency (PE) for control MG-63 monolayers and disaggregated spheroids was 35.5 and 32.0%, respectively. These control PE's were always taken into account to calculate cell survival. As can be seen in the cell survival curves for monolayers and spheroids reported in Fig. 3, both these cell models have very similar radiosensitivities. The data reported in Fig. 3 are in sharp contrast to those shown in Figs. 1 and 2 in which irradiation seems to damage monolayer cells more than spheroids with respect to both growth and nuclear morphology. In order to attempt to comprehend the reasons for these discrepancies, spheroids

Time after irradiation (h)	Monolayer		Spheroids	
	Mitotic catastrophe (%)		Apoptosis (%)	
	Control	5 Gy	Control	5 Gy
24	3.10±0.81	27.40±2.51	<1	<1
48	2.70±0.42	48.80±5.12	<1	10.70±2.51
72	3.42±0.51	64.21±6.62	2.42±0.31	28.60±6.11

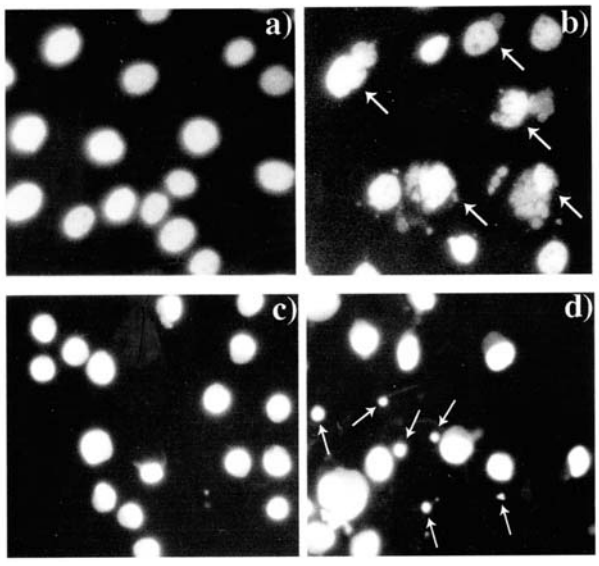

Figure 2. Analysis of cell death by Hoechst 33258 staining of MG-63 monolayer cells and spheroids at 24, 48 and 72 h after 5-Gy irradiation. The percentages of cells undergoing mitotic catastrophe or apoptosis are shown in the table. The values reported represent the means and standard deviations of three separate experiments. All differences between control and irradiated cells and spheroids are significant ($p<0.05$). Representative fluorescence micrographs of (a) control and (b) irradiated MG-63 monolayer cells at 72 h after irradiation and (c) control and (d) irradiated MG-63 spheroids collected and disaggregated at this same time point are shown. In (a) and (c), the nuclei have uncondensed and uniformly and homogeneously distributed chromatin, characteristics typical of control cells. Irradiated monolayer cells (b) reveal the typical morphology of mitotic catastrophe (i.e., multiple, multilobed or abnormally large nuclei or micronuclei, arrows), while in the disaggregated spheroid cells (d), the nuclear morphological and ultrastructural parameters typical of apoptosis (clumped or condensed nuclear chromatin, arrows) were observed. Original magnification x1000.

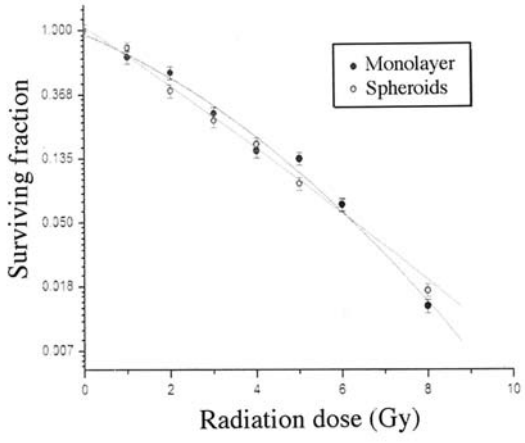

Figure 3. Survival curve of MG-63 monolayer cells and spheroids after radiation doses ranging from 1 to 8 Gy. Both cells and spheroids have very similar survival characteristics and radiosensitivities.

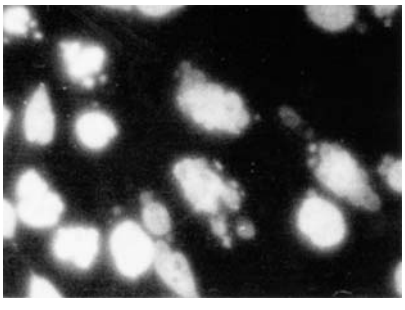

Figure 4. Hoechst 33258 stained MG-63 spheroid cells observed at 72 h after 5-Gy irradiation. Cells were disaggregated and seeded immediately after irradiation. These spheroid cells reveal the typical morphology of mitotic catastrophe as described above. Original magnification x1300.

were disaggregated immediately after the 5-Gy irradiation in the same manner as was conducted for the survival curve experiments and seeded. As can be seen in Fig. 4, 72 h after this seeding, Hoechst stained cells from spheroids have the same morphological characteristics of mitotic catastrophe as irradiated monolayer cells. Therefore, cells from spheroids disaggregated immediately after irradiation do not maintain the response to irradiation typical of spheroids, but resemble

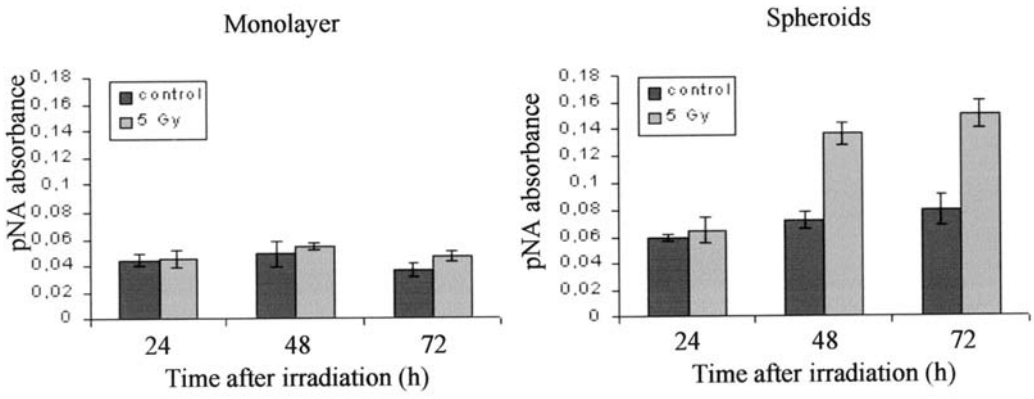

Figure 5. Caspase-3 activity (expressed in pNA absorbance at 405 nm) in control and irradiated MG-63 monolayer cells and in control and irradiated MG-63 spheroids at 24, 48 and 72 h after 5-Gy irradiation. There is no caspase-3 activation in irradiated monolayer cells at 24 and 48 h, whereas there is a very slight yet significant activation of this enzyme at 72 h ($p<0.05$). Conversely, sharp significant increases in the activation of caspase-3 are seen in spheroids at both 48 and 72 h after 5-Gy irradiation ($p<0.05$). The absorbance values represent the means and standard deviations of three separate experiments.

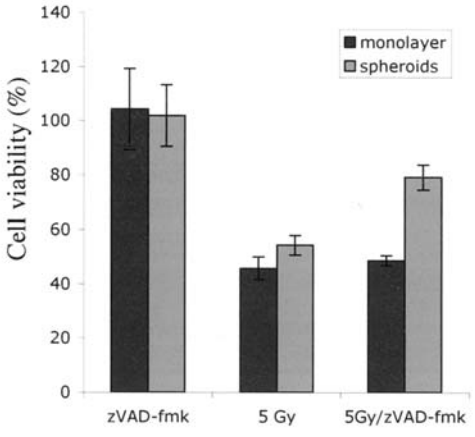

Figure 6. Histogram reporting the percentage of surviving MG-63 monolayer and spheroid cells 72 h after 5-Gy irradiation and/or after treatment with the caspase inhibitor zVAD-fmk. These percentages were calculated with respect to untreated controls. The values reported represent the means and standard deviations of three separate experiments. The zVAD-fmk did not affect the percentage of surviving monolayer cells after irradiation. Conversely, the percentage of surviving cells increased significantly in irradiated spheroids also treated with zVAD-fmk with respect to irradiated spheroids alone ($p<0.05$).

more closely the response of monolayer cells and die of mitotic catastrophe rather than by apoptosis.

Caspase-3 enzymatic activity. In order to determine if caspase-3 has been activated after irradiation with 5 Gy in the two cell models analyzed, the activity of this enzyme was determined. In Fig. 5 the increases in enzymatic activities of caspase-3 (expressed in pNA absorbance) in MG-63 monolayer cells and spheroids irradiated with 5 Gy collected at 24, 48 and 72 h after irradiation with respect to untreated controls collected at the same time-points are shown. There is no significant increase in caspase-3 activity in monolayer cells at 24 and 48 h with respect to controls whereas there is a slight yet significant increase in the enzymatic activity at 72 h ($p<0.05$). In spheroids, on the other hand, there is a sharp increase in caspase-3 activity at both 48 and 72 h ($p<0.05$).

Determination of the role of caspases in irradiation-induced cell death using the inhibitor zVAD-fmk. In order to better examine if the two types of cell death observed in MG-63 monolayer cells and spheroids are caspase-dependent, the broad-spectrum caspase inhibitor zVAD-fmk was used. As can be seen in Fig. 6, zVAD-fmk did not affect the number of surviving monolayer cells 72 h after irradiation. The percentage of surviving cells, with respect to controls, was about 46% and 49%, respectively, in irradiated monolayer cells and in irradiated cells also treated with zVAD-fmk. Conversely, in spheroids, the percentage of surviving cells increased from about 54% in those irradiated with 5 Gy to about 79% in irradiated cells also treated with zVAD-fmk ($p<0.05$). Therefore, it appears that zVAD-fmk can affect the number of surviving cells in spheroids. In addition, Hoechst staining was also used to verify the effects of zVAD-fmk in irradiated monolayer cells and spheroids. In fact, the number of cells undergoing mitotic catastrophe (Fig. 7) and apoptosis (Fig. 8) was determined 72 h after irradiation alone and after irradiation and zVAD-fmk treatment. Fig. 7 demonstrates that the percentage of cells undergoing mitotic catastrophe in monolayers is nearly the same after irradiation alone and after irradiation and zVAD-fmk treatment (both about 64%). Again, zVAD-fmk does not appear to affect the percentage of monolayer cells undergoing mitotic catastrophe. Fig. 8 shows the effects of zVAD-fmk on the number of spheroid cells undergoing apoptosis. Treatment with zVAD-fmk significantly decreases the percentage of irradiated spheroid cells undergoing apoptosis (about 29% vs about 6%), to a level approximating that of controls (about 3%). Thus, it appears that the radiation-induced apoptosis examined in MG-63 spheroids is caspase-dependent. It should be recalled that the values for mitotic catastrophe in spheroids and of apoptosis in monolayer cells are both very low (<1% and ≤4%, respectively) and therefore are not reported.

Determination of the expression of Bax, Bcl-2 and survivin by Western blot analysis. In order to evaluate the possible changes in the expression of proteins involved in cell death in response to radiation exposure, Bax, Bcl-2 and survivin

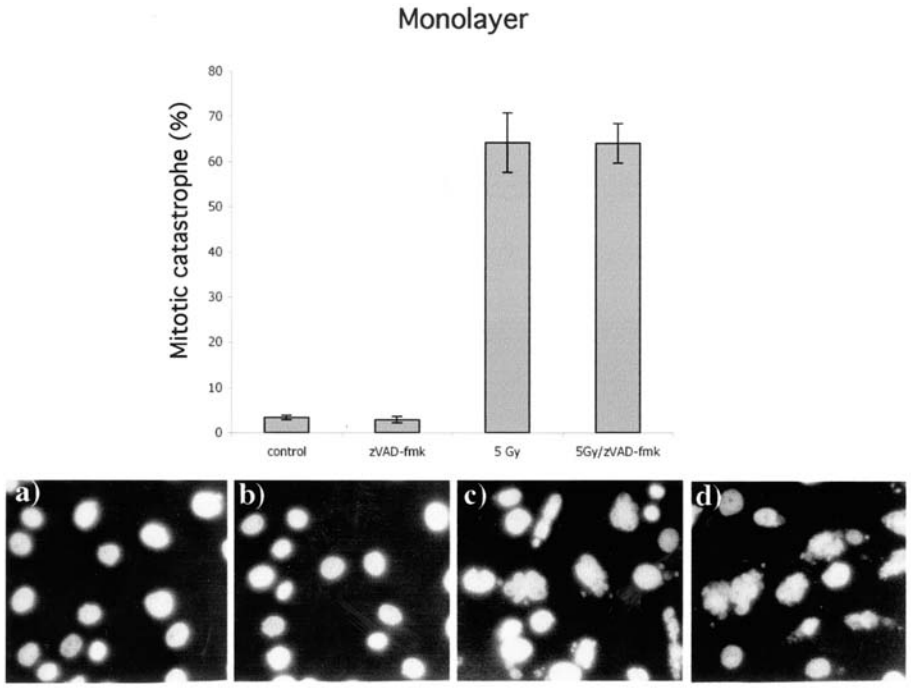

Figure 7. Analysis of the effects of zVAD-fmk in 5-Gy-irradiated monolayer cells by determination of the number of Hoechst 33258 stained cells undergoing mitotic catastrophe after irradiation alone and after irradiation and zVAD-fmk treatment. As shown in the histogram, the percentage of cells undergoing mitotic catastrophe is nearly the same after irradiation alone and after irradiation and zVAD-fmk treatment. The experiments were conducted at 72 h after irradiation and the means and standard deviations of three separate experiments are reported. Representative micrographs of control MG-63 monolayer cells (a), and monolayer cells treated with zVAD-fmk alone (b), irradiated with 5 Gy (c) and treated with zVAD-fmk and irradiated with 5 Gy (d) are shown. Original magnification x800.

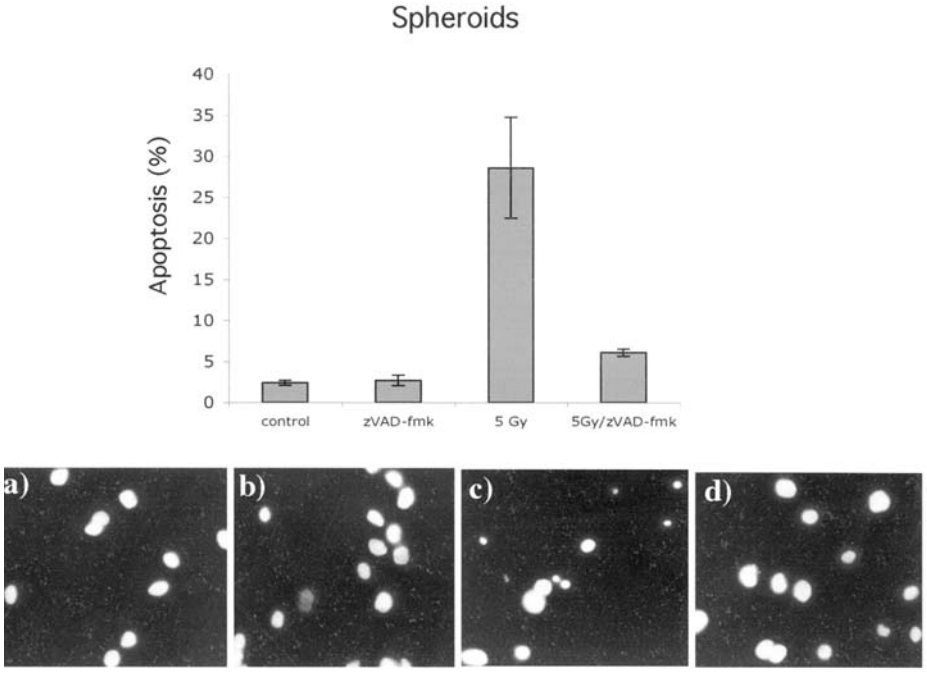

Figure 8. Analysis of the effects of zVAD-fmk in 5-Gy-irradiated spheroids by determination of the number of disaggregated Hoechst 33258 stained spheroid cells undergoing apoptosis after irradiation alone and after irradiation and zVAD-fmk treatment. As shown in the histogram, the percentage of irradiated spheroid cells undergoing apoptosis decreases sharply ($p<0.05$), reaching a level approximating that of controls when irradiation is conducted together with zVAD-fmk treatment. The experiments were conducted at 72 h after irradiation and the means and standard deviations of three separate experiments are reported. Representative micrographs of control MG-63 spheroid cells (a), and spheroid cells treated with zVAD-fmk alone (b), irradiated with 5 Gy (c) and treated with zVAD-fmk and irradiated with 5 Gy (d) are shown. Original magnification x800.

were analyzed by Western blotting. As can be seen in Fig. 9, the pro-apoptotic protein Bax increases in spheroids at 24 h after 5-Gy irradiation, whereas this protein remains unchanged in monolayer cells after the same 5-Gy irradiation. The anti-apoptotic protein Bcl-2, on the other hand, remains unchanged in both monolayer cells and spheroids. Finally, survivin

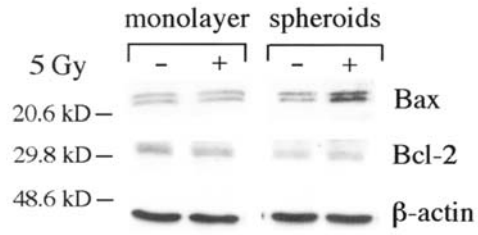

Figure 9. Western blot analysis of Bax and Bcl-2 protein expression in monolayer MG-63 cells and spheroids at 24 h after 5-Gy irradiation. The pro-apoptotic Bax protein increases in spheroids, whereas this protein remains unchanged in monolayer cells after the same 5-Gy irradiation. The anti-apoptotic protein Bcl-2, on the other hand, remains unchanged in both monolayer cells and spheroids. Experiments were repeated three times. An equal loading of proteins was confirmed by utilizing an antibody against ß-actin as control.

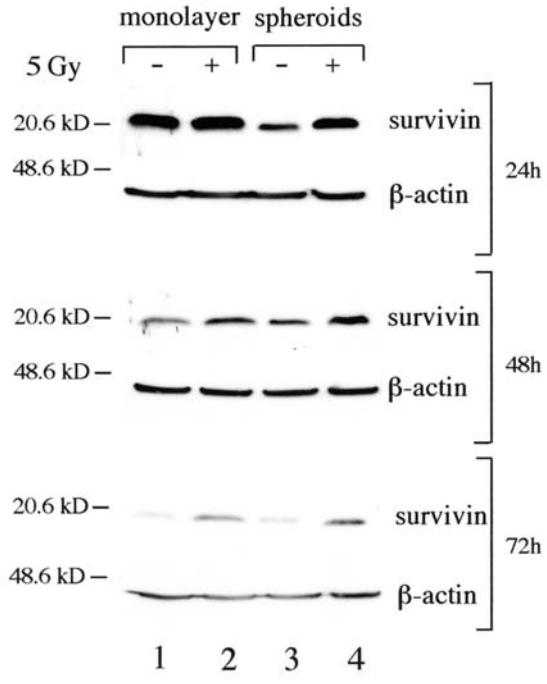

Figure 10. Western blot analysis of survivin expression in monolayer MG-63 cells and spheroids at 24, 48 and 72 h after 5-Gy irradiation. Survivin increases significantly after irradiation in both monolayers and spheroids at all the times tested. Experiments were repeated three times. An equal loading of proteins was confirmed by utilizing an antibody against ß-actin as control.

(Fig. 10) increases significantly after irradiation in both monolayers and spheroids at all the times tested.

In order to demonstrate that survivin plays a role in the radioresistance of MG-63 cells, the amount of survivin was determined using Western blot analysis in clones that had survived a 5-Gy irradiation. As shown in two representative clones in Fig. 11 (lanes 2 and 3), the amount of survivin increased in these clones when compared to unexposed control cells (lane 1).

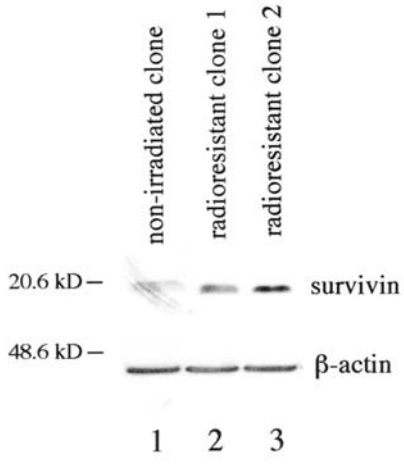

Figure 11. Western blot analysis of survivin expression in MG-63 clones that had survived 5-Gy irradiation. As shown in the two representative clones (lanes 2 and 3), the amount of survivin increases in these clones when compared to unexposed control cells (lane 1). Experiments were repeated three times. An equal loading of proteins was confirmed by utilizing an antibody against ß-actin as control.

Discussion

Three-dimensional tumor spheroids conserve many of the characteristics of early, avascular solid tumors and thus represent a useful *in vitro* model system to investigate many aspects of tumor biology. Because of their specific cell-cell and cell-matrix interactions, growth characteristics, nutrient and oxygen diffusion dynamics and the existence of heterogeneous microregions, these systems reproduce much more closely *in vivo* solid tumors than cells in monolayer. In addition, because of the strong differences from monolayer cultures, it can also be hypothesized that spheroids die in a diverse manner from these bidimensional cultures. The data reported in the present report indicate that, MG-63 monolayer cells die of mitotic catastrophe, while three-dimensional spheroids die of apoptosis after 5 Gy of ionizing radiation. Ionizing radiation is known to induce both cell death through apoptosis (7) as well as through mitotic catastrophe in different cell types (23,24).

The growth curves presented in this work provide the first indications of possible differences in the response to ionizing radiation of the two cell models examined. At all times tested after irradiation, cell number was drastically reduced in monolayers with respect to controls, whereas in spheroids, although cell number also decreased with respect to controls, this reduction was not as sharp. Differences in the response of monolayer cells and spheroids to radiation were also noted by morphological analyses of these two cell models using the chromatin dye Hoechst 33258. Irradiated monolayer cells reveal the typical morphology of mitotic catastrophe (i.e., multiple, multilobed or abnormally large nuclei or micronuclei) (9,10), while spheroids have the nuclear morphological and ultrastructural parameters typical of apoptosis (i.e., cells were considered apoptotic if their nuclei had clumped or condensed nuclear chromatin (11-13). These studies showed that not only did the two cell models die by two different types of cell death, but that monolayer cells were more damaged than spheroid cells since the number of abnormal nuclei (i.e., both apoptotic and those exhibiting the characteristics of mitotic catastrophe) were much greater in monolayer cells at all times tested. Survival

curves, on the other hand, indicated that clonogenic survival was very similar in monolayer cells and spheroids, contradicting the differences observed by growth curve determination and morphological analyses. In order to explain these contradictory results, it was hypothesized that perhaps clonogenic survival curves may not be the best manner to represent long-term survival in spheroids. It should be recalled that in order to construct these curves, spheroids must be disaggregated immediately after irradiation and seeded as a single-cell suspension. It is apparent that the cell-cell interactions, that may be responsible for the differences in cell death observed by the other techniques which maintained these important interactions, are no longer present. In order to validate this possible explanation, MG-63 spheroids were disaggregated and seeded immediately after 5-Gy irradiation and observed after 72 h. As was described above, these spheroid cells reveal the typical morphology of mitotic catastrophe and not that of apoptosis as occurs in whole spheroids. Thus, it is apparent that clonogenic survival curves cannot be used to examine long-term survival in irradiated MG-63 spheroids. Whether or not these curves are inadequate in comparing radioresistance between monolayers and spheroids formed from all cell lines needs further investigation. In this regard, it should be pointed out that other investigators have also conducted similar experiments in different cell lines (25,26). In particular, clonogenic survival curves demonstrated that the resistance of A431 squamous carcinoma cells and spheroids to ionizing radiation was the same, while it was very different in cells and spheroids of the CaSki squamous carcinoma line (25). The same resistance in monolayer cells and spheroids was also found in the Chinese hamster V79 cell line after X-irradiation (26). Therefore, in view of these considerations, it is of paramount importance that investigators keep in mind the pivotal role played by cell-cell interaction in determining radioresistance when conducting experiments with spheroids.

In order to better characterize the molecular differences between the mitotic catastrophe occurring in MG-63 monolayer cells and apoptosis taking place in spheroids of this same cell line, the role of caspases and proteins involved in the cell death response (e.g., members of the Bcl-2 family of apoptotic proteins and survivin) was determined. In order to examine if the two types of cell death observed in MG-63 monolayer cells and spheroids are caspase-dependent, caspase-3 activity was determined and the broad-spectrum caspase inhibitor zVAD-fmk was used. As was reported above, there is a slight yet significant increase in caspase-3 enzymatic activity in monolayer cells only at 72 h after irradiation. In spheroids, on the other hand, there is a sharp increase in caspase-3 activity beginning at 48 h. It should be noted that mitotic catastrophe, which can be observed using Hoechst 33258 staining by 24 h, precedes caspase-3 activation in monolayer cells suggesting that this activation is not involved in the mitotic catastrophe observed. Conversely, caspase-3 activation in spheroids can be detected by 48 h, the same culture time when apoptosis, as revealed by Hoechst 33258 staining, has also initiated. This observation indicates a possible role of caspase-3 in the apoptosis noted. In order to better elucidate the role of caspases in mitotic catastrophe and apoptosis in monolayer cells and spheroids, respectively, zVAD-fmk was used. As was reported, zVAD-fmk did not affect the number of surviving monolayer cells after irradiation nor the number of abnormal nuclei in these cells, but it did cause an increase in the number of surviving cells as well as a sharp decrease in abnormal apoptotic nuclei in spheroids. Therefore, the mitotic catastrophe in MG-63 monolayers is of the more frequently occurring caspase-independent type (14,20,27-29), although involvement of caspases has also been suggested in different cell types (30-32). MG-63 spheroids, on the other hand, die from the more classical caspase-dependent apoptosis, even if it is becoming increasingly evident that apoptosis can also proceed in a caspase-indepent manner (33,34).

Members of the Bcl-2 family of apoptotic proteins were also examined in order to better characterize the molecular differences between the mitotic catastrophe occurring in MG-63 monolayer cells and apoptosis taking place in spheroids. Although the role of Bcl-2 proteins is well-documented in the regulation of mitochondrial outer membrane permeabilization during apoptosis (35), their role in mitotic catastrophe is still controversial. A number of studies have shown that Bcl-2 proteins play a role in mitotic catastrophe (15,22), while others do not attribute such a role (14,21). In the present report, Bcl-2 and Bax were examined and only an increase in Bax was observed in MG-63 spheroids undergoing caspase-dependent apoptosis. No variations were noted in monolayer cells during caspase-independent mitotic catastrophe. These differences in Bax expression in the two cell models examined may be explained, at least in part, by the role that this protein plays in cell death. Bax itself may be caspase-dependent since it has been observed that it can be activated by caspase-9 (36). More importantly, Bax is required to activate effector caspase-3 (36,37). In accordance with this latter observation, the increase of Bax expression in irradiated MG-63 spheroids reported in this work precedes caspase-3 activation. In particular, the increase in Bax was noted already by 24 h after irradiation, while caspase-3 activation occurred 48 h after this exposure.

Survivin is overexpressed in cancer and is frequently correlated to resistance to antineoplastic therapies and to a poor prognosis (38). In addition, survivin is a bifunctional protein that controls cell division and inhibits apoptosis (16-19,39). Because of the role of survivin in G2/M and spindle checkpoint control and the importance of dys-regulation of these checkpoints in mitotic catastrophe (15), survivin can also be involved in regulating this type of cell death (20,40,41). In this study, it was shown that irradiation induced a significant increase in survivin expression in both MG-63 monolayer cells undergoing mitotic catastrophe and spheroids dying of apoptosis. It has been suggested that an increase in survivin expression is a marker for radiation resistance (42,43). Therefore, it may be hypothesized that the rise in survivin observed in this work in both cell models after irradiation may be indicative of resistance. Although there is no direct proof of this postulate, it was shown that the amount of survivin in clones that had survived 5-Gy irradiation was much higher than in unexposed control cells.

In conclusion, the results presented in this report show that MG-63 cells grown in monolayer and as spheroids respond in a different manner to 5 Gy of ionizing radiation, suggesting that three-dimensional cell organization may play a major role. A different behavior of MG-63 spheroids

with respect to monolayer cells as a consequence of three-dimensional organization was also observed using two-photon excitation microscopy (44). In this report, an increase in hypoxia-responsive elements (HRE) activity was seen in spheroids with respect to monolayer cells. It should be recalled that HRE are present in a series of genes involved in metabolic adaptation, hematopoieses, changes in adhesive and invasive properties, angiogenesis and apoptosis (45,46). Therefore, this diverse activation of the HRE sequences suggests that monolayer cells and spheroids of the MG-63 cell line have different genes turned on and thus diverse functional activities and survival characteristics. In addition, three-dimensional cell organization and the resulting increase in cell-cell interaction was also shown to play a key role in the diverse response to ionizing radiation (47). Variations in cell compaction led to either apoptosis or necrosis in HT-29 human colon adenocarcinoma spheroids exposed to ionizing radiation. Thus, it appears that the use of spheroids, a cell model that mimics *in vivo* solid tumors more closely than cells grown in monolayer, is more appropriate when investigating the effects of antineoplastic treatments such as ionizing radiation.

References

1. Santini MT and Rainaldi G: Three-dimensional spheroid model in tumor biology. Pathobiology 67: 148-157, 1999.
2. Santini MT, Rainaldi G and Indovina PL: Apoptosis, cell adhesion and the extracellular matrix in the three-dimensional growth of multicellular tumor spheroids. Crit Rev Oncol Hematol 36: 75-87, 2000.
3. Thews O, Zywietz F, Lecher B and Vaupel P: Quantitative changes of metabolic and bioenergetic parameters in experimental tumors during fractionated irradiation. Int J Radiat Oncol Biol Phys 45: 1281-1288, 1999.
4. Iliakis G, Wang Y, Guan J and Wang H: DNA damage checkpoint control in cells exposed to ionizing radiation. Oncogene 22: 5834-5847, 2003.
5. Suzuki K, Ojima M, Kodama S and Watanabe M: Radiation-induced DNA damage and delayed induced genomic instability. Oncogene 22: 6988-6993, 2003.
6. Benderitter M, Vincent-Genod L, Pouget JP and Voisin P: The cell membrane as a biosensor of oxidative stress induced by radiation exposure: a multiparameter investigation. Radiat Res 159: 471-483, 2003.
7. Watters D: Molecular mechanisms of ionizing radiation-induced apoptosis. Immunol Cell Biol 77: 263-271, 1999.
8. Santini MT, Romano R, Rainaldi G, Ferrante A, Indovina P, Motta A and Indovina PL: ^{1}H-NMR evidence for a different response to the same dose (2 Gy) of ionizing radiation of MG-63 human osteosarcoma cells and three-dimensional spheroids. Anticancer Res 26: 267-281, 2006.
9. Abend M: Reasons to reconsider the significance of apoptosis for cancer therapy. Int J Radiat Biol 79: 927-941, 2003.
10. Swanson PE, Carroll SB, Zhang XF and Mackey MA: Spontaneous premature chromosome condensation, micronucleus formation, and non-apoptotic cell death in heated HeLa S3 cells. Ultrastructural observations. Am J Pathol 146: 963-971, 1995.
11. Bär PR: Apoptosis - the cell's silent exit. Life Sci 59: 369-378, 1996.
12. Oberhammer FA, Froschl G, Tiefenbacher R, *et al*: A topical issue of microscopy research and technique. Microsc Res Tech 34: 247-258, 1996.
13. Inayat-Hussain SH, Cohen GM and Cain K: A reappraisal of the role of Zi^{++} in TGF-ß1-induced apoptosis in primary hepatocytes. Cell Biol Toxicol 15: 381-387, 1999.
14. Nabha SM, Mohammad RM, Dandashi MH, Coupaye-Gerard B, Aboukameel A, Pettit GR and Al-Katib AM: Combretastatin-A4 prodrug induces mitotic catastrophe in chronic lymphocyte leukemia cell line independent of caspase activation and poly(ADP-ribose) polymerase cleavage. Clin Cancer Res 8: 2735-2741, 2002.
15. Castedo M, Perfettini J-L, Roumier T, Andreau K, Medema R and Kroemer G: Cell death by mitotic catastrophe: a molecular definition. Oncogene 23: 2825-2837, 2004.
16. Li F, Ambrosini G, Chu EY, Plescia J, Tognin S, Marchisio PC and Altieri DC: Control of apoptosis and mitotic spindle checkpoint by survivin. Nature 396: 580-584, 1998.
17. O'Connor DS, Grossman D, Plescia J, *et al*: Regulation of apoptosis at cell division by p34cdc2 phosphorylation of survivin. Proc Natl Acad Sci USA 97: 13103-13107, 2000.
18. Lens SM, Wolthuis RM, Klompmaker R, *et al*: Survivin is required for a sustained spindle checkpoint arrest in response to lack of tension. EMBO J 22: 2934-2947, 2003.
19. Song Z, Yao X and Wu M: Direct interaction between survivin and Smac/DIABLO is essential for the anti-apoptotic activity of survivin during Taxol-induced apoptosis. J Biol Chem 278: 23130-23140, 2003.
20. Shankar SL, Sridhar M, O'Guin KN, Kandimalla ER, Agrawal S and Shafit-Zagardo B: Survivin inhibition induces human neural tumor cell death though caspase-independent and -dependent pathways. J Neurochem 79: 426-436, 2001.
21. Lock RB and Stribinskiene L: Dual modes of death induced by etoposide in human epithelial tumor cells allow Bcl-2 to inhibit apoptosis without affecting clonogenic survival. Cancer Res 56: 4006-4012, 1996.
22. Elez R, Piiper A, Kronenberger B, *et al*: Tumor regression by combination antisense therapy against Plk1 and Bcl-2. Oncogene 22: 69-80, 2003.
23. Kakizaki T, Hamada N, Wada S, *et al*: Distinct modes of cell death by ionizing radiation observed in two lines of feline T-lymphocytes. J Radiat Res 47: 237-243, 2006.
24. Ianzini F, Bertoldo A, Kosmacek EA, Phillips SL and Mackey MA: Lack of p53 function promotes radiation-induced mitotic catastrophe in mouse embryonic fibroblast cells. Cancer Cell Int 6: 11, 2006.
25. Kwok TT and Sutherland RM: The influence of cell-cell contact on radiosensitivity of human squamous carcinoma cells. Radiat Res 126: 52-57, 1991.
26. Staab A, Zukowski D, Walenta S, Scholz M and Mueller-Klieser W: Response of Chinese hamster V79 multicellular spheroids exposed to high-energy carbon ions. Radiat Res 161: 219-227, 2004.
27. Eom YW, Kim MA, Park SS, *et al*: Two distinct modes of cell death induced by doxorubicin: apoptosis and cell death through mitotic catastrophe accompanied by senescence-like phenotype. Oncogene 24: 4765-4777, 2005.
28. Jo WS, Jeong MH, Jin YH, *et al*: Loss of mitochondrial membrane potential and caspase activation enhance apoptosis in irradiated K562 cells treated with herbimycin A. Int J Radiat Biol 81: 531-543, 2005.
29. Swift ME, Wallden B, Wayner EA and Swisshelm K: Truncated RAR beta isoform enhances proliferation and retinoid resistance. J Cell Physiol 209: 718-725, 2006.
30. Castedo M, Perfettini J-L, Roumier T, *et al*: Mitotic catastrophe constitutes a special case of apoptosis whose suppression entails aneuploidy. Oncogene 23: 4362-4370, 2004.
31. Mansilla S, Priebe W and Portugal J: Mitotic catastrophe results in cell death by caspase-dependent and caspase-independent mechanisms. Cell Cycle 5: 53-60, 2006.
32. Vitale I, Antoccia A, Cenciarelli C, *et al*: Combretastatin CA-4 and combretastatin derivative induce mitotic catastrophe dependent on spindle checkpoint and caspase-3 activation in non-small cell lung cancer cells. Apoptosis 12: 155-166, 2007.
33. Donovan M and Cotter TG: Control of mitochondrial integrity by Bcl-2 family members and caspase-independent cell death. Biochim Biophys Acta 1644: 133-147, 2004.
34. Hail N Jr, Carter BZ, Konopleva M and Andreeff M: Apoptosis effector mechanisms: a requiem performed in different keys. Apoptosis 11: 889-904, 2006.
35. Martinou JC and Green DR: Breaking the mitochondrial barrier. Nat Rev Mol Cell Biol 2: 63-67, 2001.
36. Kepp O, Rajalingam K, Kimmig S and Rudel T: Bak and Bax are non-redundant during infection- and DNA damage-induced apoptosis. EMBO J 26: 825-834, 2007.
37. Perfettini J-L, Roumier T, Castedo M, *et al*: NF-kappaB and p53 are the dominant apoptosis-inducing transcription factors elicited by the HIV-1 envelope. J Exp Med 199: 620-640, 2004.
38. Altieri DC: Survivin and apoptosis control. Adv Cancer Res 88: 31-52, 2003.

39. Olie RA, Simoes-Wust AP, Baumann B, Leech SH, Fabbro D, Stahel RA and Zangemeister-Wittke U: A novel antisense oligonucleotide targeting survivin expression induces apoptosis and sensitizes lung cancer cells to chemotherapy. Cancer Res 60: 2805-2809, 2000.
40. Tu SP, Cui JT, Liston P, *et al*: Gene therapy for colon cancer by adeno-associated viral vector-mediated trasfer of survivin Cys84Ala mutant. Gastroenterology 128: 361-375, 2005.
41. Wolanin K, Magalska A, Mosieniak G, *et al*: Curcumin affects components of the chromosomal passenger complex and induces mitotic catastrophe in apoptosis-resistant Bcr-Abl-expressing cells. Mol Cancer Res 4: 457-469, 2006.
42. Chakravarti A, Zhai GG, Zhang M, *et al*: Survivin enhances radiation resistance in primary human glioblastoma cells via caspase-independent mechanisms. Oncogene 23: 7494-7506, 2004.
43. Zhang B, Pan JS, Liu JY, Han SP, Hu G and Wang B: Effects of chemotherapy and/or radiotherapy on survivin expression in ovarian cancer. Methods Find Exp Clin Pharmacol 28: 619-625, 2006.
44. Indovina P, Collini M, Chirico G and Santini MT: Three-dimensional cell organization leads to almost immediate HRE activity as demonstrated by molecular imaging of MG-63 spheroids using two-photon excitation microscopy. FEBS Lett 581: 719-726, 2007.
45. Harris AL: Hypoxia - a key regulatory factor in tumor growth. Nat Rev Cancer 2: 38-47, 2002.
46. Carmeliet P, Dor Y, Herbert JM, *et al*: Role of HIF-1α in hypoxia-mediated apoptosis, cell proliferation and tumour angiogenesis. Nature 394: 485-490, 1998.
47. Ferrante A, Rainaldi G, Indovina P, Indovina PL and Santini MT: Increased cell compaction can augment the resistance of HT-29 human colon adenocarcinoma spheroids to ionizing radiation. Int J Oncol 28: 111-118, 2006.